JOURNAL OF PROTEOMICS 113 (2015) 315–325

Available online at www.sciencedirect.com

ScienceDirect

www.elsevier.com/locate/jprot

A proteomic analysis of p53-independent induction of apoptosis by bortezomib in 4T1 breast cancer cell line

Azmi Yerlikaya[a,*], Emrah Okur[b], Ahmet Tarık Baykal[c], Ceyda Acılan[d], İhsan Boyacı[e], Engin Ulukaya[f]

[a]Dumlupınar University, Faculty of Medicine, Department of Medical Biology, Kütahya, Turkey
[b]Dumlupınar University, Art and Science Faculty, Department of Biology, Kütahya, Turkey
[c]İstanbul Medipol University, Medical School, Department of Medical Biochemistry, İstanbul, Turkey
[d]TÜBİTAK, MAM, Genetic Engineering and Biotechnology Department, Gebze, Kocaeli, Turkey
[e]İstanbul Medipol University, Vatan Clinic, İstanbul, 34214, Turkey
[f]Department of Medical Biochemistry, Uludağ University, Bursa, Turkey

ARTICLE INFO

Article history:
Received 27 March 2014
Accepted 15 September 2014
Available online 8 October 2014

Keywords:
Apoptosis
Bortezomib
Cancer
Proteasome
Proteomics
Ubiquitin

ABSTRACT

The 26S proteasome is a proteolytic enzyme found in both cytoplasm and nucleus. In this study, we examined the differential expression of proteasome inhibitor bortezomib-induced proteins in p53-deficient 4T1 cells. It was found that GRP78 and TCEB2 were over-expressed in response to treatment with bortezomib for 24 h. Next, we analyzed the expression of intracellular proteins in response to treatment with 100 nM bortezomib for 24 h by label-free LC-MS/MS. These analyses showed that Hsp70, the 26S proteasome non-ATPase regulatory subunit 14 and sequestosome 1 were increased at least 2 fold in p53-deficient 4T1 cells. The proteins identified by label-free LC-MS/MS were then analyzed by Ingenuity Pathway Analysis (IPA) Tool to determine biological networks affected by inhibition of the 26S proteasome. The analysis results showed that post-translational modifications, protein folding, DNA replication, energy production and nucleic acid metabolism were found to be among the top functions affected by the 26S proteasome inhibition. The biological network analysis indicated that ubiquitin may be the central regulator of the pathways modulated after bortezomib-treatment. Further investigation of the mechanism of the proteins modulated in response to the proteasomal inhibition may lead to the design of more effective and novel therapeutic strategies for cancer.

Biological significance
Although the proteasome inhibitor bortezomib is approved and used for the treatment of human cancer (multiple myeloma), the mechanism of action is not entirely understood. A number of studies showed that proteasome inhibitors induced apoptosis through upregulation of tumor suppressor protein p53. However, the role of tumor suppressor protein p53 in bortezomib-induced apoptosis is controversial and not well-understood. The tumor suppressor p53 is mutated in at least 50% of human cancers and is strongly induced by proteasomal

* *Corresponding author*. Tel.: +90 274 265 2031.
E-mail address: azmiyerlikaya@yahoo.com (A. Yerlikaya).

http://dx.doi.org/10.1016/j.jprot.2014.09.010

inhibition. Some also reported that the proteasome inhibitor can induce apoptosis in a p53-independent manner. Also, it is reported that Noxa, a target of p53, is induced in response to proteasomal inhibition in a p53-independent manner. However, we have also previously reported that neither Puma nor Noxa are induced by proteasomal inhibition in p53-*null* 4T1 breast cancer cells, which is commonly used for in vivo breast cancer tumor models. The current results provided additional targets of proteasome inhibitor bortezomib and may therefore help in understanding the p53-independent mechanism of apoptosis induction by proteasome inhibitors. In addition, the results presented in this current study report for the first time that proteasomal subunit Psmd14, anti-apoptotic GRP78, anti apoptotic protein Card10, Dffb, Traf3 and Trp53bp2 are regulated and overexpressed in response to proteasome inhibitor bortezomib in p53-deficient 4T1 cells. Therefore, novel therapeutic strategies targeting these anti-apoptotic or pro-apoptotic proteins as well as inhibiting the proteasome simultaneously may be more effective against cancer cells. The proteins identified here present new avenues for the development of anti-cancer drugs.

1. Introduction

The 26 proteasome is a multi-functional enzyme found in the cytosol and nucleus as well as in the outer surface of the endoplasmic reticulum [1]. Since its first discovery in 1987 by Hough and colleagues [2], a large amount of accumulated evidence showed that the proteasome was not simply involved in the degradation of misfolded and mutated proteins but also involved in almost all intracellular processes, including DNA repair, transcription, protein synthesis, polyamine biosynthesis and antigen presentation by regulated degradation of a wide range of short- and long-lived proteins [3–5]. While the 26S proteasome primarily degrades ubiquitinated proteins [6], it may also degrade proteins (e.g., ornithine decarboxylase) in a ubiquitin-independent manner [7].

The 26S proteasome has at least 3 different proteolytic activities. These are 1) chymotrypsin-like activity, 2) trypsin-like activity and 3) caspase-like activity [8,9]. As mentioned above, the 26S proteasome plays critical roles in almost all biological processes; therefore, aberrations in the proteasomal system are implicated in the pathogenesis of many diseases, including cancer [3]. In fact, Hoffmann et al. recently showed that circulating proteasome concentrations were significantly higher in primary breast cancer patients than in healthy controls. They therefore concluded that the ubiquitin–proteasome system might represent a potential target in breast cancer treatment [10]. The activity of the proteasome as well as the levels of the proteasome subunits were also increased in at least 90% of the primary breast cancer tissue specimens; whereas, no significant increases in the proteasome activity or the levels of its subunits were observed in benign breast tumors [11]. In contrast to these studies, Pan et al. showed that the chymotrypsin-like and caspase-like activities of the proteasome were significantly lower in lung tumor spheres as compared to monolayer cultures [12]. Interestingly, they confirmed that the population of tumor cells with low proteasomal activity were highly enriched for cancer stem cells in sphere cultures using the ZsGreen–cODC reporter assay [12].

A number of studies demonstrated that proteasome inhibitors have anti-proliferative and pro-apoptotic effects against both hematological and solid tumors [13]. For example, carfilzomib, an irreversible inhibitor of chymotrypsin-like activity of the proteasome, is effective against hematological and solid tumors and is currently in Phase III trials in multiple myeloma and Phase I trials for acute myeloid leukemia, acute lymphoblastic leukemia, chronic lymphocytic leukemia and solid tumors [14]. Another inhibitor, bortezomib, also known as Velcade™ or PS-341, is a highly potent and reversible inhibitor of the 26S proteasome [15,16]. Bortezomib is the first inhibitor entered into clinical trials and was approved in 2003 by the FDA for the treatment of multiple myeloma and for relapsed or refractory mantle cell lymphoma [5,17,18]. A vast number of studies showed that bortezomib-induced apoptotic cell death in both a p53-dependent and a p53-independent manner [19,20], and exposure to bortezomib is known to cause the stabilization/accumulation or activation of a number of regulatory or pro-apoptotic proteins such as p21, p53, p27, caspase-3, Bid and Bax [20–22]. Valeniner et al. also showed that bortezomib-treatment not only has pro-apoptotic effects but also anti-mitotic, anti-antigiogenic and anti-metastatic effects in a SCID mouse model [23]. In order to further delineate the mechanism of p53-independent induction of apoptosis after proteasomal inhibition, we examined the differential expression of proteins in response to bortezomib-treatment by proteomic techniques in p53-deficient 4T1 breast cancer cell, which is commonly used for in vivo breast cancer tumor models. After 2-dimensional gel electrophoresis (2-DE) analysis, 10 different proteins spots were identified by LC-MS/MS analysis in 4T1 cells treated with bortezomib. Among these proteins are 78 kDa glucose regulated protein, cytochrome B5 type B, transcription elongation factor B and galectin-1. Using label-free LC-MS/MS analysis, 345 proteins were identified in 4T1 cells and the expressions of 107 proteins were statistically changed. In addition, using real time PCR measurements, it was found for the first time that inhibition of the 26S proteasome by bortezomib causes upregulation of Card10, Dffb, Traf3 and Trp53bp2 genes; however, Bcl2l1, Fadd, Traf1 and Xiap genes were downregulated. The increases in the levels of Card10 and Trp53bp2 proteins were confirmed by Western blot analysis.

2. Materials and methods

2.1. Materials

ZOOM 2D protein solubilizer, complete protease inhibitor cocktail, ZOOM carrier ampholytes pH 3–10, ZOOM strips—

pH 3–10NL, NuPAGE LDS sample buffer, NuPAGE Novex 4–12% Bis-Tris ZOOM gels and SilverQuest™ silver staining kit were obtained from Invitrogen Life Technologies, Inc. (CA, USA). The Amersham ECL Western blotting kit and Bio-Rad protein assay reagents were purchased from GE Healthcare (Stockholm, Sweden). RPMI-1640 media, FBS, trypsin, Pen/Strep and Bio-Max X-ray film were bought from Sigma-Aldrich Inc., (Steinheim, Germany). The Stericup vacuum filtration system (0.2 μm) and PVDF membrane were from Millipore Inc. (St-Quentin, France). The rabbit anti-GRP78 (C-terminal) antibody and rabbit anti-LGALS1 (galectin-1) antibody were from Sigma-Aldrich Inc., (Steinheim, Germany). Anti-TCEB2 antibody was from Santa Cruz Biotechnology (Heidelberg, Germany). Rabbit polyclonal β-actin was obtained from Abcam (Cambridge, UK). Bortezomib was obtained from Pharmacy of Uludağ University Medical School Hospital (Bursa, Turkey).

2.2. Cell culture maintenance

The cell line used in this study (4T1 breast cancer) was cultured in RPMI-1640 (plus 4.5 g/l glucose, 10 mM HEPES, 1 mM sodium pyruvate, 0.15% sodium bicarbonate, 100 μg/ml streptomycin and 100 U/ml penicillin). The medium was supplemented with 10% FBS. Stock cultures were maintained in 25 cm^2 Corning flasks. For the experiments, the cells were grown in 35 × 10 mm Corning plates. The cells were subcultured when they reached to about 70% confluency.

2.3. 2-dimensional (2D) gel electrophoresis

2D gel electrophoresis was carried out according to the protocol of Invitrogen Life Technologies Inc. Briefly, cells (4T1) were grown in 60 × 15 mm petri dishes and treated with 100 nM bortezomib at the logarithmic phase of growth for 24 h. After washing with PBS, cells were detached with 909 μl ZOOM 2-D protein solublizer I, 3 μl 1 M tris-base, 10 μl 100X protease inhibitor cocktail, 10 μl 2 M DDT and 18 μl dH_2O and lyzed completely by an ultrasonicator. After protein quantitation with Bio-Rad method, Zoom IPG strip (pH3–10NL strip) were rehydrated with 140 μl sample rehydration buffer (128 μl 1X ZOOM 2-D protein solublizer I, 0.7 μl 2 M DDT, 0.8 μl ZOOM carrier ampholytes, 0.5 μl bromophenaol blue and 10 μl cell lysate containing 90 μg protein) for 1 h at room temperature. The isoelectric focusing (IEF) was performed at 175 V for 15 min, 175–2000 V gradient for 45 min and finally 2000 V for 30 min. Afterwards, IEF gels were reduced with 1X NuPAGE LDS sample buffer containing NuPAGE sample reducing agent for 15 min, and then were alkylated with 1X NuPAGE LDS sample buffer containing iodoacetamide for 15 min. Zoom IPG strips were placed in NuPAGE 4–12% Bis-Tris ZOOM gel wells and covered with 400 μl %0.5 agarose solution. Proteins were then separated according to their molecular weights at 200 V for 50 min. To visualize the protein spots, SilverQuest silver staining kit was used according to the manufacturer's protocol (Invitrogen Life Technologies Inc.). Protein spots which showed increased levels compared to the control gel were excised and destained according to the procedure of the manufacturer (Invitrogen Life Technologies Inc.). Enzymatic digestion was then performed with trypsin (12.5 ng/μL) in 10 nM ammonium bicarbonate buffer (pH 7.8) overnight. The tryptic peptides were extracted by washing the gel slices with 10 nM ammonium bicarbonate and 1% formic acid in 50% acetonitrile at room temperature and then analyzed by LC-MS/MS as described in detail below.

2.4. Proteomics analysis

4T1 breast cancer cells were treated with 100 nM bortezomib at the logarithmic phase of the growth for 24 h. After exposure to bortezomib, cells were detached and pelleted at 700 ×*g* for 5 min. The cell pellets were then lysed via boiling at 100 °C in UPX Buffer (Expedeon, UK). Tryptic peptides were generated according to the Filter Aided Sample Preparation Protocol (FASP) [24]. Briefly, 50 μg protein was first washed with 6 M urea in a 30 kDa cut-off spin column and then alkylated with 10 mM iodoactamide (IAA) in the dark for 20 min at room temperature and trypsinized overnight (1:100 trypsin to protein ratio). Peptides were eluted from the column and concentration was measured with a nanodrop spectrometer. 500 ng total tryptic peptide spiked with 50 fmol internal standard (MassPREP Enolase Digestion Standard, Waters, Milford, MA) was injected to the LC-MS/MS system. Protein Lynx Global Server software was used for the identification of the protein spots digested with trypsin. This software uses a Monte Carlo algorithm to analyze all available MS data and is also a statistical data for the accuracy of assignation [25,26]. PLGS Score calculated by the Protein Lynx Global Server (PLGS 2.2.5) software is a statistical measure of accuracy of assignation. A higher score indicates greater confidence of protein identity. The cut off (threshold) for the PLGS score was 20 (same cut off was used in a previous published study) [27]. Databank search query was set to minimum 3 fragment ion matches per peptide, minimum 7 fragment ion matches per protein, minimum 1 peptide matches per protein and 1 missed cleavage. The status of the b and y ions for each identified peptide was also manually inspected. The false positive rate (FPR) of the Identity^E algorithm is around 3–4% [28] for the randomized database with being five times larger than the original one [29]. As reported in the protein identification (Table 1) almost all of the proteins were identified with more than one peptide sequence, increasing the protein identification score greatly. All proteins with PLGS score >20 (at least 95% confident) were counted as confidently identified.

2.5. LC-MS/MS analysis and database search

Protein identification is based on a previously published protocol [30]. Briefly, 500 ng tryptic peptides were analyzed by the LC-MS/MS system (nanoACQUITY UPLC and SYNAPT high definition mass spectrometer with nanolockspray ion source). Columns were equilibrated with 97% mobile phase A (0.1% formic acid in LC-MS grade water (Merck, NJ, USA) and column temperature was set to 45 °C. Peptides were separated from the trap column (Symmetry C18 5 μm, 180 μm i.d. × 20 mm) (Waters, Milford, MA) by gradient elution onto an analytical column (BEH C18, 1.7 μm, 75 μm i.d. × 250 mm) (Waters, Milford, MA) at 300 nl/min flow rate with a linear gradient from 5 to 40% mobile phase B (0.1 formic acid in hypergrade acetonitrile (Merck, NJ, USA) over 90 min. All samples were analyzed in triplicate. Data independent

Table 1 – The identification of protein spots on 2-DE. The cells were treated with 100 nM bortezomib for 24 h. After separation on 2-DE, nine protein spots (annotated in Fig. 1B) up-regulated were excited and analyzed by LC-MS/MS. PLGS Score is calculated by the Protein Lynx Global Server (PLGS 2.2.5) software and is a statistical measure of accuracy of assignation. A higher score implies greater confidence of protein identity. It should be noted that the experimental peptide number exceeds the theoretical peptide number (e.g., for GRP78); that is partly due to the fact that some peptides were detected multiple times because of either modified forms (such as oxidation, deamination, carbamidomethyl C) or missed cleavages or non-tryptic cut sites that would cause different overlapping versions of the same theoretical peptides to be counted to a total higher than the "theoretical number of tryptic peptides."

Spot	Accession	Protein	M.W. (dalton)	pI	PLGS score	Peptides [a]	Theoretical [b]	Coverage (%) [c]
1	P63242	Eukaryotic translation initiation factor 5A (eIF5A)	16821	4.9	685	1	14	15.5
2	Q9CQX2	Cytochrome b5 type B (CYB5B)	16307	4.6	5641	7	11	58.9
3	Q3THE2	Myosin regulatory light chain 12B (MYL12B)	19766	4.5	7783	16	19	54.6
4	P62869	Transcription elongation factor polypeptide 2 B (TCEB2)	13161	4.7	3964	9	15	55.9
	Q9CR41	Huntingtin interacting protein K (HYPK)	14670	4.7	769	3	12	31
	Q9CQL7	MORF4 family associated protein 1(MRFAP1)	14185	4.5	483	4	10	24.8
5	P16045	Galectin 1 (Gal-1)	14856	5.1	378	3	14	25.9
6	P17742	Peptidyl prolyl cis trans isomerase A (PPlaseA)	17959	8	15876	37	12	83.5
7	O09172	Glutamate cysteine ligase regulatory subunit (GCLM)	30515	5.2	1130	9	18	28.8
8	P56480	ATP synthase subunit beta mitochondrial (ATP5B)	56265	5	580	25	37	19.6
9	P20029	78 kDa glucose regulated protein (GRP78)	72377	4.9	24566	122	52	66
10	P63017	Heat shock cognate 71 kDa protein (HSPA8)	70827	5.2	30901	174	50	70.4

[a] The experimental number of peptides which are identified with more than three fragment ion matches.
[b] The theoretical number of peptides in each protein.
[c] The percentage of sequence coverage

acquisition mode (MS^E) was done by operating the instrument at positive ion V mode, applying the MS and MS/MS functions over 1.5 s intervals with 6 V low energy and 15–40 V high energy collusion. Glu-fibrinopeptide (internal mass calibrant) was infused at 300 nl/min flow rate. *m/z* values over 50–1600 were analyzed. Tandem mass data extraction, charge state deconvolution and deisotoping were done with ProteinLynx Global Server v2.5 (Waters, Milford, MA) and searched with the $IDENTITY^E$ algorithm with a fragment ion mass tolerance of 0.025 Da and a parent ion tolerance of 0.0100 Da against the reviewed mouse protein database from Uniprot (March 30th 2012, 30419 entries). Carbamidomethyl-cysteine fixed modification and Acetyl N-TERM, deamidation of asparagine and glutamine, and oxidation of methionine variable modifications were set. Quantification of the protein expression changes was done with Progenesis LC-MS software V4.0 (Nonlinear Dynamics). Normalization across samples were based on total ion intensity. Similar proteins were group and quantitative value is given for the one with the highest score. Protein quantitation is done with only the non-conflicting peptide features. For LC-MS/MS study, three distinct biological samples were used and each sample was analyzed in triplicate. Therefore, nine separate injections were made for each biological group.

2.6. Western blot analysis

The ECL Western blotting kit was used according to manufacturer procedure (GE Healthcare, Stockholm, Sweden). A total of 50 μg protein from each sample was separated on a 12% SDS-PAGE. Afterwards, proteins were transferred to PVDF membranes at 70 V for 2 h. After the transfer, the PVDF membranes were washed briefly with methanol and left for drying for 15 min to enhance the protein binding. The PVDF membranes were again reactivated by methanol. The membranes were blocked by 5% non-fat dried milk in TBS-T. The membranes were then incubated with anti-GRP78 antibody (1:750 dilution), anti-TCEB2 (1:500) and anti-galectin-1 antibody (1:1000 dilution). For loading control, the membranes were probed with anti-β-actin antibody (1:5000) in TBS-T for 1 h. The membranes were then incubated with HRP-conjugated anti-rabbit secondary antibody (1:5000 dilution) in TBS-T for 1 h. Finally, the membranes were incubated with detection reagent and exposed to Kodak BioMax X-ray films in dark room.

2.7. Bioinformatic analysis

Proteins identified by label-free LC-MS/MS were analyzed by the Ingenuity Pathway Analysis Tool (IPA, Ingenuity Systems, Redwood City, CA) for biological functions, associated diseases and biological networks. Right-tailed Fisher's exact test was used to determine a *p*-value indicating that the probability of biological functions, canonical pathways and diseases associated with the networks is because of chance alone. The IPA tool also computes a score for each network according to the fit of the set of significant gene products. The score is derived from a *p*-value, and scores of 2 or higher have at least a 99% confidence of not being generated by random chance alone.

3. Results

The 26S proteasome inhibitors are able to induce apoptosis through both p53-dependent and p53-independent mechanisms [19,20]. To examine the p53-independent induction of apoptosis, we have previously examined the expression of a number of proteins such as Puma, Noxa and Bad in 4T1 breast cancer cells. However, no significant changes in the levels of these proteins were detected [20]. We have also previously reported that cancer cells are differentially sensitive to

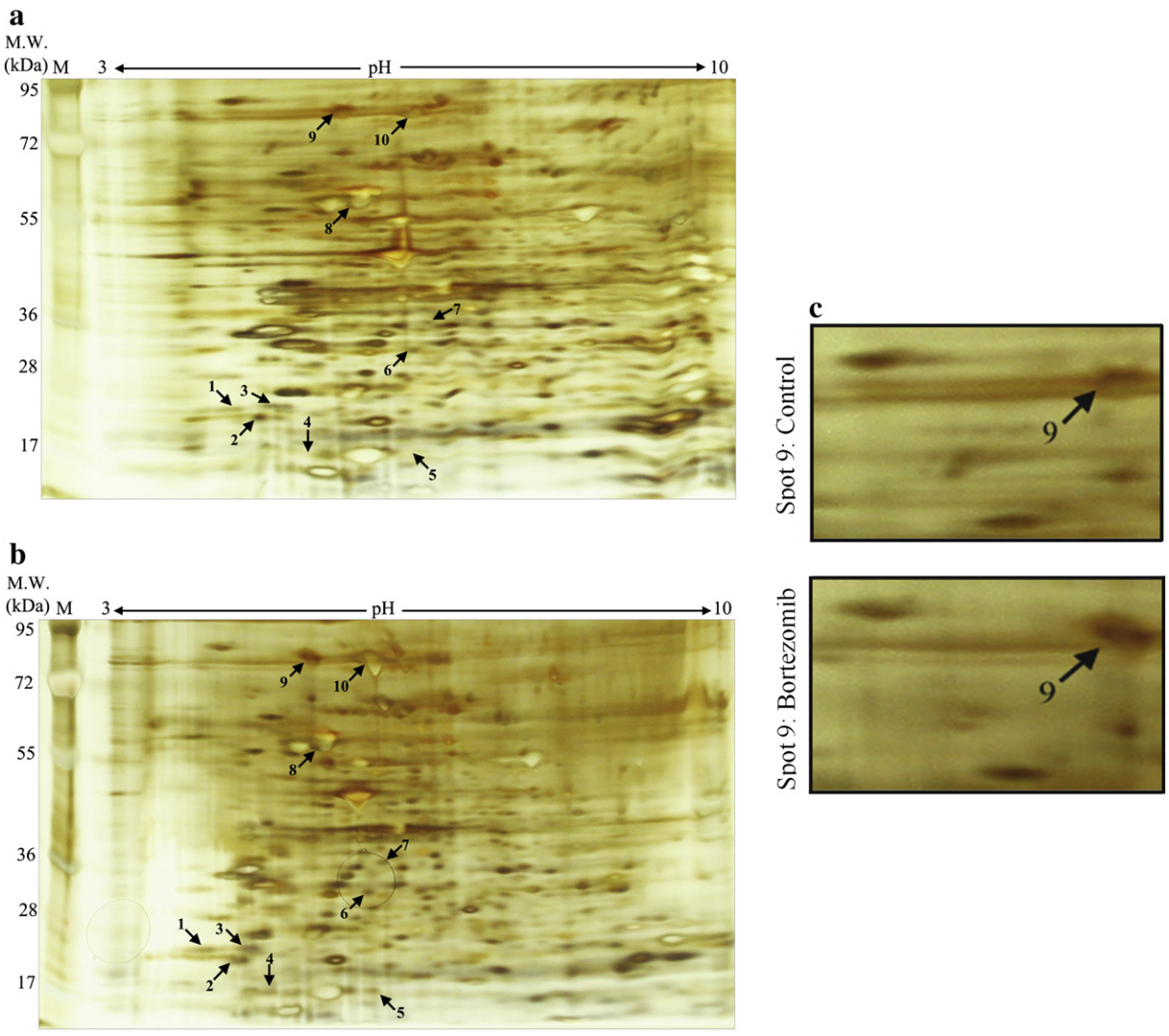

Fig. 1 – 2-DE analysis of effect of bortezomib in 4T1 cells. A) Control cells were treated with vehicle (isotonic solution) for 24 h. Then 90 μg proteins were separated on pH 3-10NL strips followed by separation on a 4-12% Bis-Tris ZOOM gel. The protein spots were visualized by silver staining. B) Cells were treated with 100 nM bortezomib for 24 h and then the proteins were analyzed by 2-DE as described. C) A zoomed image of spot 9 (GRP78). The panel shows the level of spot 9 in control (isotonic solution treated) and bortezomib-treated cells (100 nM).

proteasomal inhibition [31]. In addition, it was previously unambiguously determined that 4T1 breast carcinoma cells are p53-*null* cells [20,31,32]. Therefore, to delineate the sensitivity or resistance of cancer cells to proteasome inhibitors in detail, we first treated p53-deficient 4T1 breast cancer cells with 100 nM bortezomib for 24 h. The changes in the expression levels of proteins were then analyzed by 2-DE and LC-MS/MS. As can be seen in Fig. 1, over 400 protein spots were clearly detected, and ten proteins showing at least 2-fold higher levels in 100 nM bortezomib-treated cells compared to control cells were selected for subsequent analysis by LC-MS/MS for protein identification. The proteins identified are listed in Table 1 and their relevant positions in the 2-DE are annotated in Fig. 1A and B. Spot 9 was identified as a 78 kDa glucose regulated protein (GRP78), whose expression is associated with tumor development and resistance to chemotherapeutic agents [33]. A zoomed image of spot 9 is shown in Fig. 1C. The analysis of spot 9 intensity by GelQuantNET program indicated that there was at least a 2 fold increase in GRP78 level upon proteasome inhibitor bortezomib-treatment as compared to that in the control cells (Fig. 1C). The raw data for all GRP78 peptides detected by nLC-MS/MS as well as a representative spectrum for the peptide with highest score showing *b* fragment ions and y fragment ions can be seen in Supplementary Table S1. The expression of GRP78 under the conditions of proteasomal inhibition was also verified by Western blot analysis following treatment of 4T1 breast cancer cells with 10 nM and 100 nM bortezomib for 24 h. As can be seen in Fig. 2A (*upper panel*), GRP78 levels were increased very significantly after inhibition of the proteasome. We have also tried to corroborate the expression of galectin-1, which has recently been described as promoting lung cancer metastasis by potentiating Notch1 and integrin signaling pathways [34]. Contrary to our expectations, there was no increase in the relative expression of galectin-1, but a decrease in its mobility in 12% SDS-PAGE was observed, which may be due to a post-translational modification (e.g.,

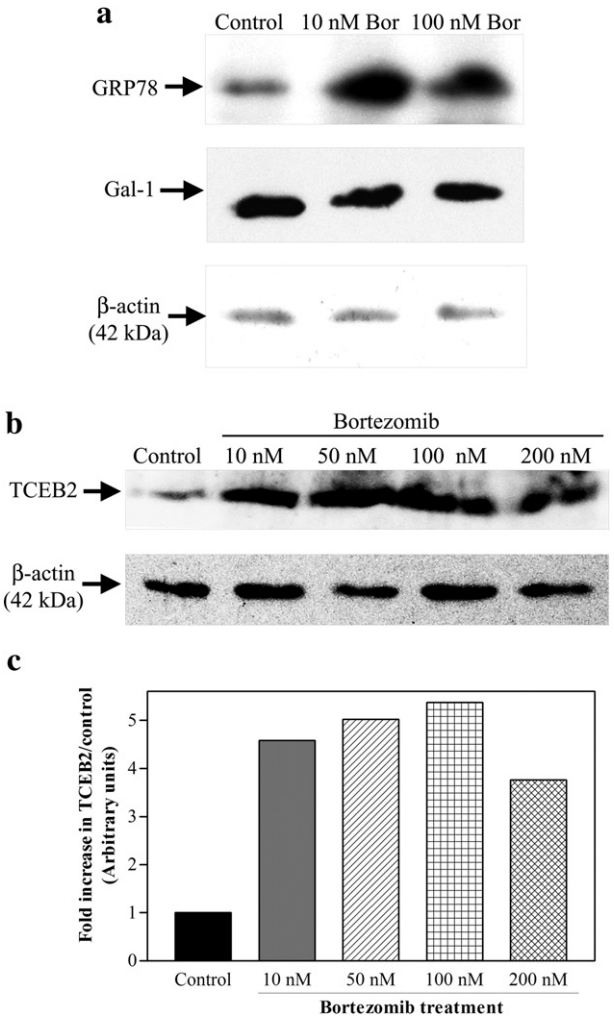

Fig. 2 – A) Western blot analysis of GRP78 and galectin-1. Cells (4T1) were treated with 10 nM and 100 nM for 24 h. Then a total of 50 μg protein was separated on 12% SDS-PAGE followed by detection with anti-GRP78 antibody (1:750 dilution), anti-TCEB2 (1:3000) or anti-galectin-1 antibody (1:1000). The membranes were then probed with HRP-conjugated secondary antibody (1:4000) for 1 h, and exposed to a film in a dark room for 2 min. B) Determination of the level of TCEB2 in response various concentrations of bortezomib. Cells were treated with 10, 50, 100 and 200 nM bortezomib for 24 and the level of TCEB2 was examined by Western blot using 25 μg of total protein. Rabbit anti-TCEB2 (1:500 dilution) was used. The blots are representative of two independent experiments each run in duplicates. C) Quantitation of the membrane shown in panel B by GelQuantNET.

phosphorylation) in response to proteasomal inhibition (Fig. 2A, *middle panel*). Therefore, the spot 5, observed in bortezomib-treated cells but not in the control cells in 2-DE gels, may be a modified form of galectin-1. Western blot analysis confirmed that transcription elongation factor B polypeptide 2 (TCEB2), a general transcription elongation factor, was induced significantly in a threshold-dependent-manner in response to treatment with bortezomib for 24 h (Fig. 2B, *upper panel*). As can be seen in Fig. 2C, the level of TCEB2 is increased in a threshold-dependent manner. In 10 nM, 50 nM and 100 nM bortezomib-treated cells, 4.6 fold, 5 fold and 5.4 fold increases in TCEB2 level were observed as compared to the control cells, respectively. These results suggest that the effect of bortezomib was already maximal at the lowest dosage tested, (i.e., 10 nM). On the other hand, the increase in 200 nM treated cells was lower than that observed with 10 nM, 50 nM or 100 nM bortezomib-treated cells, but it was still 3.8 fold higher than that in control cells. The decrease in the level of TCEB2 protein as compared to 10 nM, 50 nM and 100 nM bortezomib-treated cells may be due to the higher toxicity of bortezomib, causing necrotic cell death in addition to the apoptosis (Fig. 2C).

Next, to further examine the differential accumulation of proteins in response to proteasomal inhibition, 4T1 cells were similarly treated with 100 nM bortezomib for 24 h. The down-regulated and up-regulated proteins were then identified by label-free analysis as described in "Materials and methods." 284 proteins were identified by a label-free LC-MS/MS analyses ($n = 3$, each sample was analyzed in triplicate); and Table 2 shows a summary of proteins consistently up-regulated or down-regulated in response to 100 nM bortezomib-treatment. Among these, Hsp70, 26S proteasome non ATPase regulatory subunit 14 and sequestosome 1 were increased at least 2-fold as compared with control ($p < 0.05$ in all cases). In contrast, 40S ribosomal protein S10, peptidyl prolyl cis trans isomerase B, unconventional myosin Ic and 3 hydroxyacyl CoA dehydrogenase type 2 were down-regulated by more than 50% in bortezomib-treated cells as compared to vehicle-treated control cells ($p < 0.05$, Table 2). In order to determine the networks and biological functions associated with the identified proteins that were differentially expressed in response to 100 nM bortezomib-treatment, the data were further analyzed using the Ingenuity Pathway Analysis (IPA) software. IPA is an online application based on published literature, establishing biological networks, canonical pathways and diseases most relevant to the identified proteins that are significantly expressed in different experimental groups. The data were fit to three networks with scores of 31, 16 and 3. A score greater than or equal to 2 gives 99% confidence that the network is not created by random chance. While the highest scoring network 1 included 12 of 20 of the identified proteins, the following network 2 and network 3 included 7 and 1 focus molecules, respectively. A merge of all three networks showing the protein–protein interactions between upregulated (in red), downregulated (in green) and not user specified proteins (in white) is shown in Fig. 3A. In our analyses, post-translational modifications ($p = 2.93 \times 10^{-7}$–1.97×10^{-2} with 5 focus molecules), protein folding ($p = 2.93 \times 10^{-7}$ with 3 focus molecules), DNA replication, recombination, and repair ($p = 2.26 \times 10^{-6}$–4.56×10^{-2} with 8 focus molecules), energy production ($p = 2.26 \times 10^{-6}$–1.78×10^{-2} with 8 focus molecules) and nucleic acid metabolism ($p = 2.26 \times 10^{-6}$–9.94×10^{-4} with 6 focus molecules) were found to be among the top functions affected in response to treatment with 100 nM bortezomib for 24 h (Fig. 3B).

To further investigate the effect of proteasome inhibitor bortezomib on other target proteins in p53-*null* 4T1 breast carcinoma cell line, real-time PCR experiment was carried out to detect the changes in the expression of genes involved in the induction of apoptosis. We therefore examined the changes in the expression of 84 apoptosis-related genes using RT^2 profiler apoptosis PCR array, highly reliable and sensitive gene

Table 2 – Label-free analysis of differential expression of proteins in response to bortezomib-treatment. Cells were treated with 100 nM bortezomib for 24 h. Then equal amounts of proteins were analyzed by label-free method. The confidence score is a significance score generated by Progenesis QI software. The statistical significance was determined by one-way ANOVA at $p < 0.05$ ($n = 3$, each sample was analyzed in triplicate).

Accession	Protein	Peptides	Confidence score	Anova p-value	Fold change
P63017	Heat shock cognate 71 kDa protein (HSPA8)	70 (1)	545	3.13e−009	1.50
P07901	Heat shock protein HSP 90 alpha (HSP90AA1)	55 (6)	357	3.70e−012	1.54
P17879	Heat shock 70 kDa protein 1B (HSPA1B)	36 (1)	278	1.1e−016	4.37
Q64524	Histone H2B type 2 E (Hist2h2be)	9 (1)	52.6	4.22e−006	0.66
P52293	Importin subunit alpha-2 (Kpna2)	9	51.9	1.70e−013	1.40
P84228	Histone H3 2 (Hist1h3b)	34 (3)	149	7.66e−004	0.63
O88685	26S protease regulatory subunit 6A (Psmc3)	5	44.5	6.66e−016	1.58
O35593	26S proteasome non ATPase regulatory subunit 14 (Psmd14)	3	36.4	5.22e−015	2.15
Q64337	Sequestosome 1 (Sqstm1)	3	29	7.77e−016	2.81
Q6R0H7	Guanine nucleotide-binding protein G(s) subunit alpha isoforms XLas (Gnas)	2	22.4	1.67e−015	1.78
P63325	40S ribosomal protein S10 (Rps10)	2 (1)	15.4	3.73e−004	0.55
Q9Z2U1	Proteasome subunit alpha type 5 (Psma5)	3 (2)	15	4.38e−013	1.56
P24369	Peptidyl prolyl cis trans isomerase B (PPlase B)	2 (1)	14.4	3.34e−007	0.49
O09061	Proteasome subunit beta type 1 (Psmb1)	1	8	6.38e−007	1.42
Q9CQQ7	ATP synthase subunit b mitochondrial (ATP5F1)	1	7.9	8.48e−007	0.63
P62245	40S ribosomal protein S15a (RPS15a)	1	14.8	8.19e−003	0.74
Q9R1P3	Proteasome subunit beta type 2 (Psmb2)	1	7.8	5.56e−010	1.47
Q8BMS1	Trifunctional enzyme subunit alpha mitochondrial (Hadha)	1	7	2.63e−011	0.69
Q9WTI7	Unconventional myosin Ic (Myo1c)	1	7	2.82e−009	0.56
O08756	3 Hydroxyacyl CoA dehydrogenase type 2 (Hsd17b10)	1	6.9	2.12e−008	0.51

expression profiling technology. As can be seen in Table 1 in Ref. [47], we have found that eleven genes were upregulated at least 2-fold using RT^2 profiler apoptosis PCR array. The degree of up-regulation varied between 2.06 fold (for Trp53bp2 gene) to 5.2 fold (for Card10 gene). In addition, four genes were found consistently downregulated in response to treatment with bortezomib for 24 h. The genes downregulated were Bcl2-like 1, Fas (TNFRSF6)-associated via death domain, Tnf receptor-associated factor 1 and X-linked inhibitor of apoptosis proteins (Table 1 in Ref. [47]). Using Western blot analysis, the increases in Card10 (Fig. 1A in Ref. [47], *upper panel*) and Trp53bp2 (Fig. 1A in Ref. [47], *middle panel*) proteins were corroborated in response to proteasomal inhibition by various concentrations of bortezomib for 24 h. The examination of β-actin level (Fig. 1A in Ref. [47], *lower panel*) showed that the changes in the protein levels of Card10 and Trp53bp2 were not simply due to higher protein loading. As can be seen in Fig. 1B in Ref. [47], when the cells were treated with different doses of bortezomib, a threshold-dependent increase in Card10 protein was clearly observed. With 10 nM, 50 nM, 100 nM and 200 nM, 1.84 fold, 2.31 fold, 2.26 fold and 3.78 fold increases were detected, respectively. On the other hand, the increase in the level of Trp53bp2 protein was observed with only higher doses of bortezomib (i.e., 100 nM and 200 nM) (Fig. 1B in Ref. [47]). With lower doses of bortezomib, slight decreases in Trp53bp2 protein were observed, which may be due to an experimental artifact (Fig. 1B in Ref. [47]). These data are in agreement with the RT-PCR measurements.

4. Discussion

It has been reported by different groups that proteasome inhibitors are versatile in inducing apoptosis in either a p53-dependent or a p53-independent manner [19,20,35]. However, despite a number of promising in vitro and in vivo studies, the efficacy of proteasome inhibitor bortezomib-therapy is hampered by drug resistant phenotypes [36]. For example, Richardson et al. reported that the response to bortezomib was 35% in patients with relapsed multiple myeloma [37]. Furthermore, breast, melanoma and head and neck cancer cell lines are differentially sensitive to bortezomib-treatment in vivo and in vitro models as well as in murine xenografts [31,38]. In this current study, we studied the p53-independent induction of apoptosis in p53-deficient 4T1 breast cancer cells following bortezomib-treatment using 2-DE and label-free LC-MS/MS proteomic techniques. Ten protein spots in 2-DE up-regulated were identified using LC-MS/MS. Among these were, for example, anti-apoptotic protein GRP78, eukaryotic translation initiation factor 5A, transcription elongation factor B, ATP synthase subunit beta mitochondrial and galectin-1. The up-regulations of GRP78 and TCEB2 were verified by Western blot analysis; on the other hand, rather than an increase in the total amount of galectin-1, we observed a decrease in the mobility of galectin-1 in SDS-PAGE, suggesting that the proteasomal inhibition causes a post-translation modification (e.g., phosphorylation) in galectin-1, which has not been reported before. The changes in the level of GRP78, cofilin-1 and heat shock cognate 71 kDa protein in relation to the proteasomal system were previously identified in different cancer cell lines or primary cells [31,39,40]. However, to our best knowledge, this is the first study showing that inhibition of the proteasome causes changes in the amount of eukaryotic translation initiation factor 5A, cytochrome b5 type B, myosin regulatory light chain 12B, transcription elongation factor B polypeptide 2, peptidyl prolyl cis trans isomerase A, calpain small subunit 1, glutamate cysteine ligase regulatory subunit and ATP synthase subunit beta mitochondrial.

We also examined the changes in the level of proteins by label-free LC-MS/MS analysis, which showed that a number of proteins involved in protein folding (e.g., heat shock proteins)

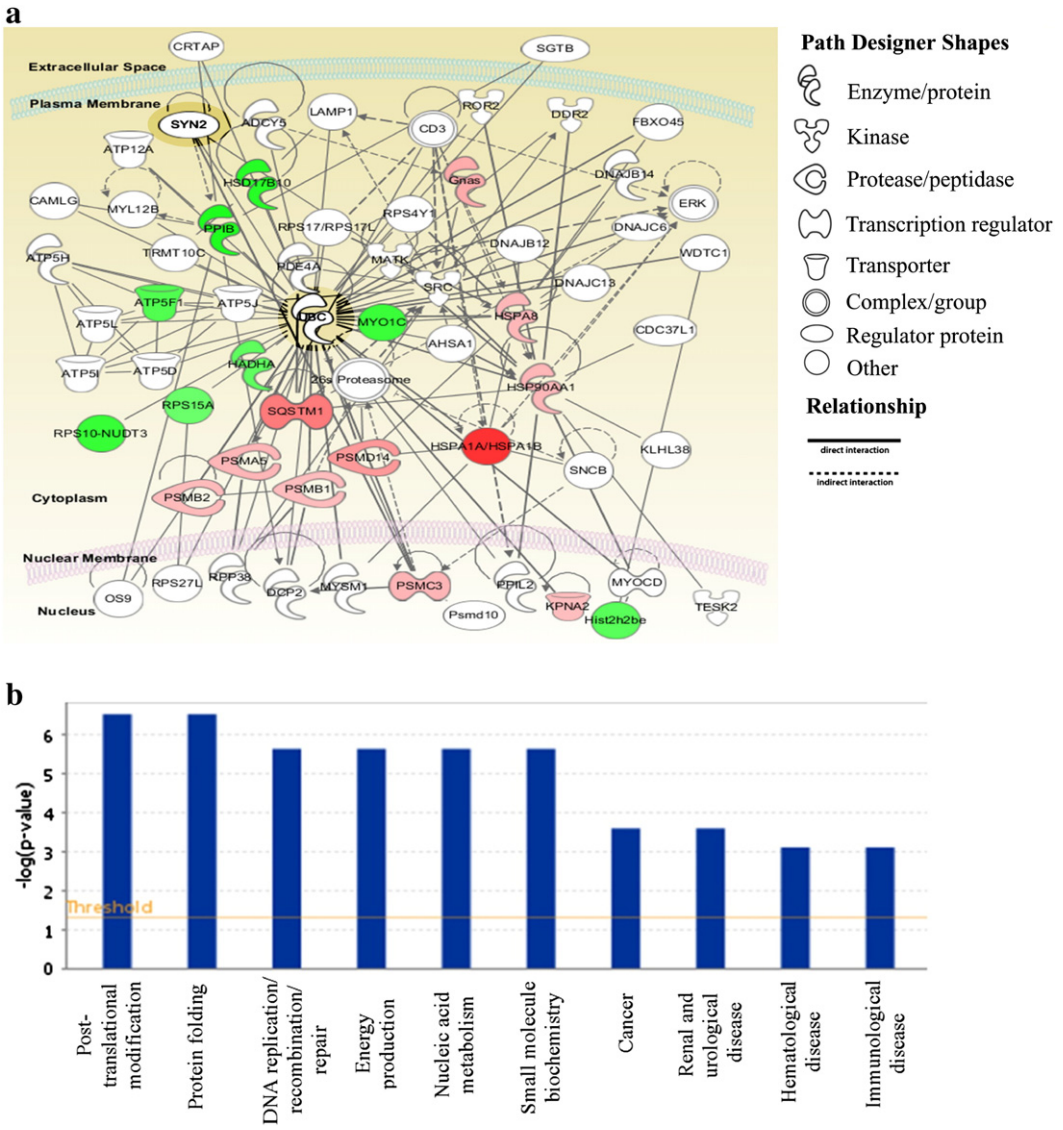

Fig. 3 – A) A merged network view of protein interactions determined by IPA software. The proteins determined by LC-MS/MS were analyzed by Ingenuity Pathway Analysis Tool. Red colored nodes show the proteins upregulated, green nodes show downregulated proteins, and white nodes are proteins not determined by label-free but with the evidence of interaction with bortezomib-regulated proteins in IPA database. B) Biological functions identified by IPA Tool. The biological functions and associated diseases were analyzed for their significant level by *p*-values calculated with Fisher's exact test. The threshold line corresponds to $p < 0.05$.

are significantly induced in response to proteasome inhibitor bortezomib. The overexpression of heat shock proteins in response to proteasome inhibitor MG-132 or bortezomib was reported in a number of studies [20,31,41]. Interestingly, a number of proteins involved in the ubiquitin-proteasome system and/or protein catabolic processes were also significantly up-regulated after treatment with bortezomib. This negative feedback regulation to proteasome inhibitors may also form the basis of drug resistant phenotypes. We have also previously shown that proteasome inhibition causes 50–60% inhibition of the protein synthesis activity through activation of heme-regulated inhibitor kinase (HRI) [22]. These results presented here also suggest that the decrease in protein synthesis activity may be partly due to the down-regulation of the structural constituents of ribosomal subunits such as 40S ribosomal protein S10. The label-free LC-MS/MS analysis also indicated for the first time that importin subunit alpha-2, Gnas (guanine nucleotide-binding protein G(s) subunit alpha isoforms XLas) and sequestosome 1 were up-regulated in response to proteasome inhibitor bortezomib. Interestingly, Myeku et al. previously showed that prolonged autophagy inhibition in cortical neurons increased the level of sequestosome 1, which was degraded mainly by autophagy and not by the proteasome. In addition, they provided strong evidence that sequestosome 1 associates with proteasomes [42]. The mechanism of increase in sequestosome 1 in response to proteasomal inhibition observed in this study needs to be further investigated and may help clarify the link between the autophagy and proteasomes. As seen in Fig. 3A and B, bortezomib-mediated inhibition of

the proteasome affected changes in the expression of proteins involved in post-translational modification, protein folding, DNA replication/repair/recombination, energy production and nucleic acid metabolism using IPA software. The role of the 26S proteasome in protein folding/chaperone system, post-translation modifications (e.g., NF-κB activation) and DNA replication/recombination/repair processes has been described before [43–45]. The merged network showed that ubiquitin (UBC gene encoding polyubiquitin-C, a precursor of ubiquitin protein) interacts with almost all proteins in the network. Interestingly, the proteasomal subunit Psmd14, a critical subunit for the development of stem cells as well, is found to be in direct contact with heat shock 70 kDa protein 1B, heat shock cognate 71 kDa, Psmc3 (a proteasomal subunit involved in diseases of meningitis and HIV-1) and also ubiquitin. Also, Psmc3 interacts directly with Syn2 protein, which is involved in synaptogenesis and the modulation of neurotransmitter release, suggesting a potential role in several neuropsychiatric diseases [46]; therefore the 26S proteasome may also be involved in neurotransmitter release and thus neuropsychiatric diseases through the interactions of proteasomal subunits with proteins like Syn2 (Fig. 3A). As can be seen in Tables 1 and 2, heat shock cognate 71 kDa protein and ATP synthase subunit beta mitochondrial were detected by two different techniques (i.e., 2D-gel electrophoresis nLC-MS/MS and label-free nLC-MS/MS); the other proteins detected are either in the same pathway (that is, protein synthesis or heat shock) or are isozymes of the same protein (e.g., peptidyl prolyl cis trans isomerase A and peptidyl prolyl cis trans isomerase B). However, the reasons for not entirely overlapping between the protein lists obtained by the two different analyses may be due to the different technical preparations of samples and analysis parameters of two independent techniques applied (i.e., 2D-gel electrophoresis nLC-MS/MS and label-free nLC-MS/MS). In addition, not all proteins can be easily detected and quantitated, due to differences in sequence composition and relative ionization efficiency of different peptides in MS.

Using real-time PCR analysis, eleven apoptosis-related genes were detected as upregulated in response to 100 nM bortezomib-treatment. The increased expression of Card10, Dffb, Traf3 and Trp53bp2 in response to inhibition of the 26S proteasome has not been reported previously. Moreover, four genes were found to be downregulated after bortezomib-treatment; these genes were Bcl2l1 (also known as Bcl-XL, an anti-apoptotic protein), Fadd, Traf1 and Xiap (which is a member of the inhibitor of apoptosis family of proteins, IAPs). It is thus likely that the proteasomal inhibition triggers the apoptotic cascade through not only increased up-regulation of pro-apoptotic proteins, but also through downregulation of anti-apoptotic proteins such as Bcl2l, Traf1 and Xiap. Furthermore, as can be seen in Table 2 and Table 1 in Ref. [47], the expressions of Hsp90 genes were determined to be significantly upregulated by both label-free MS/MS and RT-PCR.

5. Conclusions

Collectively, the results presented here indicate that the proteasome is involved in the degradation/modification of a significant number of proteins, each of which plays critical roles in various intracellular processes. The results presented above indicate that bortezomib-mediated inhibition of the proteasome altered the expression of proteins involved in post-translational modification, protein folding, protein synthesis, transport, transcription, DNA replication/repair/recombination, energy production, autophagy and programmed cell death. In addition, the network analysis indicated that the proteasome may also be involved in neurotransmitter release and thus neuropsychiatric diseases. Therefore, an in-depth investigation and identification of the mechanism of the ubiquitin-proteasome pathway may lead to more effective and novel therapeutic strategies for cancer patients harboring either mutant p53 or wild-type p53.

Supplementary data to this article can be found online at http://dx.doi.org/10.1016/j.jprot.2014.09.010.

Conflict of interest

The authors of the study entitled “A proteomic analysis of p53-independent induction of apoptosis by bortezomib in 4T1 breast cancer cell line” declare that there are no conflicts of interest.

Acknowledgment

This study was financially supported by the Scientific and Technological Research Council of Turkey (TÜBİTAK) with Project no SBAG 109S035. We are grateful to Dr. Bruce A. Stanley (Pennsylvania State University, College of Medicine) for critical reading and suggestions during the preparation of the manuscript.

REFERENCES

[1] Wojcik C, DeMartino GN. Intracellular localization of proteasomes. Int J Biochem Cell Biol 2003;35(5):579–89.
[2] Hough R, Pratt G, Rechsteiner M. Purification of two high molecular weight proteases from rabbit reticulocyte lysate. J Biol Chem 1987;262(17):8303–13.
[3] Lecker SH, Goldberg AL, Mitch WE. Protein degradation by the ubiquitin–proteasome pathway in normal and disease states. J Am Soc Nephrol 2006;17(7):1807–19.
[4] Yerlikaya A, Stanley BA. S-adenosylmethionine decarboxylase degradation by the 26 S proteasome is accelerated by substrate-mediated transamination. J Biol Chem 2004;279(13):12469–78.
[5] Yerlikaya A, Yontem M. The significance of ubiquitin proteasome pathway in cancer development. Recent Pat Anticancer Drug Discov 2013;8(3):298–309.
[6] Finley D. Recognition and processing of ubiquitin–protein conjugates by the proteasome. Annu Rev Biochem 2009;78:477–513.
[7] Murakami Y, Matsufuji S, Kameji T, Hayashi S, Igarashi K, Tamura T, et al. Ornithine decarboxylase is degraded by the 26S proteasome without ubiquitination. Nature 1992;360(6404):597–9.
[8] Burger AM, Seth AK. The ubiquitin-mediated protein degradation pathway in cancer: therapeutic implications. Eur J Cancer 2004;40(15):2217–29.

[9] Frankland-Searby S, Bhaumik SR. The 26S proteasome complex: an attractive target for cancer therapy. Biochim Biophys Acta 2012;1825(1):64–76.
[10] Hoffmann O, Heubner M, Anlasik T, Winterhalter M, Dahlmann B, Kasimir-Bauer S, et al. Circulating 20S proteasome in patients with non-metastasized breast cancer. Anticancer Res 2011;31(6):2197–201.
[11] Chen L, Madura K. Increased proteasome activity, ubiquitin-conjugating enzymes, and eEF1A translation factor detected in breast cancer tissue. Cancer Res 2005;65(13): 5599–606.
[12] Pan J, Zhang Q, Wang Y, You M. 26S proteasome activity is down-regulated in lung cancer stem-like cells propagated in vitro. PLoS One 2010;5(10):e13298.
[13] Crawford LJ, Walker B, Irvine AE. Proteasome inhibitors in cancer therapy. J Cell Commun Signal 2011;5(2):101–10.
[14] Kuhn DJ, Orlowski RZ, Bjorklund CC. Second generation proteasome inhibitors: carfilzomib and immunoproteasome-specific inhibitors (IPSIs). Curr Cancer Drug Targets 2011;11(3):285–95.
[15] Adams J. The proteasome: a suitable antineoplastic target. Nat Rev Cancer 2004;4(5):349–60.
[16] Field-Smith A, Morgan GJ, Davies FE. Bortezomib (Velcade®) in the treatment of multiple myeloma. Ther Clin Risk Manag 2006;2(3):271–9.
[17] Buac D, Shen M, Schmitt S, Kona FR, Deshmukh R, Zhang Z, et al. From Bortezomib to other Inhibitors of the proteasome and beyond. Curr Pharm Des 2013;19(22):4025–38.
[18] Orlowski RZ, Kuhn DJ. Proteasome inhibitors in cancer therapy: lessons from the first decade. Clin Cancer Res 2008; 14(6):1649–57.
[19] Lopes UG, Erhardt P, Yao R, Cooper GM. p53-dependent induction of apoptosis by proteasome inhibitors. J Biol Chem 1997;272(20):12893–6.
[20] Yerlikaya A, Okur E, Ulukaya E. The p53-independent induction of apoptosis in breast cancer cells in response to proteasome inhibitor bortezomib. Tumour Biol 2012;33(5): 1385–92.
[21] Boccadoro M, Morgan G, Cavenagh J. Preclinical evaluation of the proteasome inhibitor bortezomib in cancer therapy. Cancer Cell Int 2005;5(1):18.
[22] Yerlikaya A, Kimball SR, Stanley BA. Phosphorylation of eIF2alpha in response to 26S proteasome inhibition is mediated by the haem-regulated inhibitor (HRI) kinase. Biochem J 2008;412(3):579–88.
[23] Valentiner U, Haane C, Nehmann N, Schumacher U. Effects of bortezomib on human neuroblastoma cells in vitro and in a metastatic xenograft model. Anticancer Res 2009;29(4): 1219–25.
[24] Wisniewski JR, Zougman A, Nagaraj N, Mann M. Universal sample preparation method for proteome analysis. Nat Methods 2009;6(5):359–62.
[25] Rosenegger D, Wright C, Lukowiak K. A quantitative proteomic analysis of long-term memory. Mol Brain 2010;3:9.
[26] Wright C, Edelmann M, diGleria K, Kollnberger S, Kramer H, McGowan S, et al. Ankylosing spondylitis monocytes show upregulation of proteins involved in inflammation and the ubiquitin proteasome pathway. Ann Rheum Dis 2009;68(10): 1626–32.
[27] Cockman ME, Webb JD, Kramer HB, Kessler BM, Ratcliffe PJ. Proteomics-based identification of novel factor inhibiting hypoxia-inducible factor (FIH) substrates indicates widespread asparaginyl hydroxylation of ankyrin repeat domain-containing proteins. Mol Cell Proteomics 2009;8(3): 535–46.
[28] D'Aguanno S, D'Alessandro A, Pieroni L, Roveri A, Zaccarin M, Marzano V, et al. New insights into neuroblastoma cisplatin resistance: a comparative proteomic and meta-mining investigation. J Proteome Res 2011;10(2):416–28.
[29] Vissers JP, Langridge JI, Aerts JM. Analysis and quantification of diagnostic serum markers and protein signatures for Gaucher disease. Mol Cell Proteomics 2007; 6(5):755–66.
[30] Hacariz O, Sayers G, Baykal AT. A proteomic approach to investigate the distribution and abundance of surface and internal Fasciola hepatica proteins during the chronic stage of natural liver fluke infection in cattle. J Proteome Res 2012; 11(7):3592–604.
[31] Yerlikaya A, Erin N. Differential sensitivity of breast cancer and melanoma cells to proteasome inhibitor Velcade. Int J Mol Med 2008;22(6):817–23.
[32] Wang H, Mohammad RM, Werdell J, Shekhar PV. p53 and protein kinase C independent induction of growth arrest and apoptosis by bryostatin 1 in a highly metastatic mammary epithelial cell line: In vitro versus in vivo activity. Int J Mol Med 1998;1(6):915–23.
[33] Delie F, Petignat P, Cohen M. GRP78 protein expression in ovarian cancer patients and perspectives for a drug-targeting approach. J Oncol 2012;2012:468615.
[34] Hsu YL, Wu CY, Hung JY, Lin YS, Huang MS, Kuo PL. Galectin-1 promotes lung cancer tumor metastasis by potentiating integrin alpha6beta4 and Notch1/Jagged2 signaling pathway. Carcinogenesis 2013;34(6):1370–81.
[35] Strauss SJ, Higginbottom K, Juliger S, Maharaj L, Allen P, Schenkein D, et al. The proteasome inhibitor bortezomib acts independently of p53 and induces cell death via apoptosis and mitotic catastrophe in B-cell lymphoma cell lines. Cancer Res 2007;67(6):2783–90.
[36] Oerlemans R, Franke NE, Assaraf YG, Cloos J, van Zantwijk I, Berkers CR, et al. Molecular basis of bortezomib resistance: proteasome subunit beta5 (PSMB5) gene mutation and overexpression of PSMB5 protein. Blood 2008;112(6):2489–99.
[37] Richardson PG, Barlogie B, Berenson J, Singhal S, Jagannath S, Irwin D, et al. A phase 2 study of bortezomib in relapsed, refractory myeloma. N Engl J Med 2003;348(26):2609–17.
[38] Chen Z, Ricker JL, Malhotra PS, Nottingham L, Bagain L, Lee TL, et al. Differential bortezomib sensitivity in head and neck cancer lines corresponds to proteasome, nuclear factor-kappaB and activator protein-1 related mechanisms. Mol Cancer Ther 2008;7(7):1949–60.
[39] Doll D, Sarikas A, Krajcik R, Zolk O. Proteomic expression analysis of cardiomyocytes subjected to proteasome inhibition. Biochem Biophys Res Commun 2007;353(2):436–42.
[40] Wang HQ, Du ZX, Zhang HY, Gao DX. Different induction of GRP78 and CHOP as a predictor of sensitivity to proteasome inhibitors in thyroid cancer cells. Endocrinology 2007;148(7): 3258–70.
[41] Grossin L, Etienne S, Gaborit N, Pinzano A, Cournil-Henrionnet C, Gerard C, et al. Induction of heat shock protein 70 (Hsp70) by proteasome inhibitor MG 132 protects articular chondrocytes from cellular death in vitro and in vivo. Biorheology 2004;41(3–4):521–34.
[42] Myeku N, Figueiredo-Pereira ME. Dynamics of the degradation of ubiquitinated proteins by proteasomes and autophagy: association with sequestosome 1/p62. J Biol Chem 2011;286(25):22426–40.
[43] Berke SJ, Paulson HL. Protein aggregation and the ubiquitin proteasome pathway: gaining the UPPer hand on neurodegeneration. Curr Opin Genet Dev 2003;13(3):253–61.
[44] Dolcet X, Llobet D, Encinas M, Pallares J, Cabero A, Schoenenberger JA, et al. Proteasome inhibitors induce death but activate NF-kappaB on endometrial carcinoma cell lines and primary culture explants. J Biol Chem 2006;281(31): 22118–30.
[45] Lin CP, Ban Y, Lyu YL, Liu LF. Proteasome-dependent processing of topoisomerase I-DNA adducts into DNA double strand breaks at arrested replication forks. J Biol Chem 2009; 284(41):28084–92.

[46] Cruceanu C, Alda M, Nagy C, Freemantle E, Rouleau GA, Turecki G. H3K4 tri-methylation in synapsin genes leads to different expression patterns in bipolar disorder and major depression. Int J Neuropsychopharmacol 2013;16(2):289–99.

[47] Yerlikaya A, Okur E, Baykal AT, Acılan C, Boyacı İ, Ulukaya E. Data for a proteomic analysis of p53-independent induction of apoptosis by bortezomib. Data in Brief 2014. http://dx.doi.org/10.1016/j.dib.2014.09.003 (in press).